Organic & Biomolecular Chemistry

PAPER

View Article Online
View Journal | View Issue

CrossMark click for updates

Cite this: *Org. Biomol. Chem.*, 2016, **14**, 10031

A red fluorophore comprising a borinate-containing xanthene analogue as a polyol sensor†

N. Shimomura,[a] Y. Egawa,*[a] R. Miki,[a] T. Fujihara,[b] Y. Ishimaru[c] and T. Seki[a]

Received 6th August 2016,
Accepted 27th September 2016

DOI: 10.1039/c6ob01695b

www.rsc.org/obc

A xanthene derivative containing a borinate moiety emitted red fluorescence with a high quantum yield. The interaction between the borinate and a sugar molecule induced a fluorescence change based on the change in the HOMO–LUMO gap. The response was pH-resistant in a wide range. In addition, catechol quenched through photoinduced electron transfer. The red fluorescence and polyol binding ability of dyes will pave the way for new biological applications of chemical sensors.

Introduction

Borinic acids are a class of organoboron compounds comprising two B–C bonds and one B–O bond. Borinic acids can coordinate with OH^- to form borinates containing two B–C bonds and two B–O bonds.[1–3] Borinates show affinity to adjacent diols, as boronic acids and boronates. Boronic acids have been widely used as sugar receptors for developing chemical sugar sensors;[4–7] borinates have been neglected from this perspective due to the difficulty in designing a system that can obtain a signal change through an ester formation between a borinate and sugar. Although there are some strategies for boronic acid-based sensors such as internal charge transfer (ICT),[7–9] photoinduced electron transfer (PET),[10,11] fluorescence resonance energy transfer,[12] excimer[13] and exciplex,[14] these systems have never been utilised to develop a sugar sensor including a borinate.

In this article, we have reported a new strategy to create a sugar sensor by incorporating a borinate moiety into a xanthene skeleton (Fig. 1a). Interestingly, the xanthene derivative shows an absorption maximum (Abs_{max}) above 600 nm, which is longer than pyronin Y (PY), a corresponding xanthene dye,[15] and shows red fluorescence with a high quantum yield. The xanthene derivative was named JoSai-Red (JS-R) after Josai University, Saitama University and its fluorescent colour.

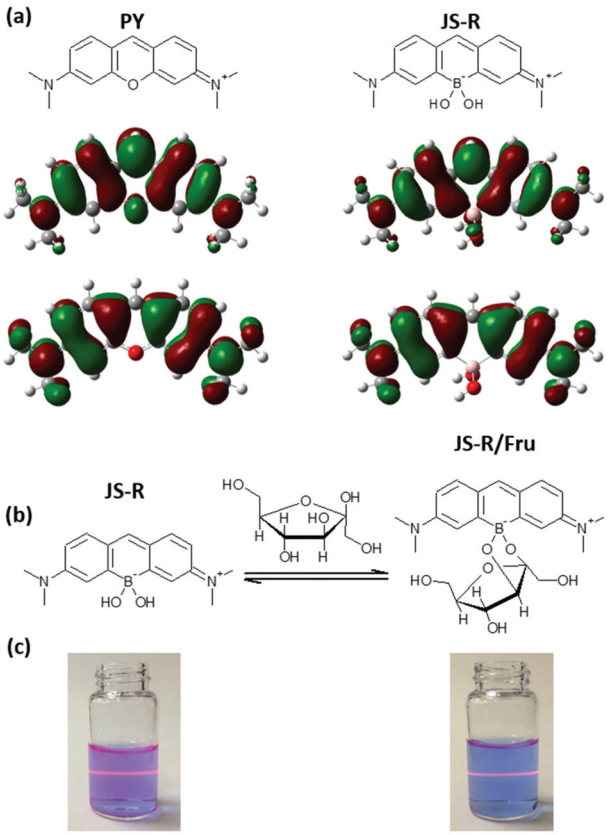

Fig. 1 (a) Chemical structures of PY and JS-R, and the DFT calculation results of their HOMO and LUMO. (b) Equilibrium of JS-R and Fru. (c) Aqueous buffered solutions (10 mM HEPES, pH 7.4) irradiated by a 532 nm laser, the left containing 6.3 μM JS-R, and the right containing 6.3 μM JS-R and 100 mM Fru.

Interaction between JS-R and sugars induced a change in the absorption and fluorescence spectra of JS-R by changing the LUMO shape (Fig. 1). In addition, interaction between JS-R

[a]*Faculty of Pharmaceutical Sciences, Josai University, 1-1 Keyakidai, Sakado, Saitama 350-0295, Japan. E-mail: yegawa@josai.ac.jp*
[b]*Research and Development Bureau, Comprehensive Analysis Center for Science, Saitama University, Shimo-ohkubo 255, Sakura-ku, Saitama, Saitama 338-8570, Japan*
[c]*Division of Material Science, Graduate School of Science and Engineering, Saitama University, 255 Shimo-ohkubo, Sakura-ku, Saitama, Saitama, 338-8570, Japan*

†Electronic supplementary information (ESI) available: Materials, apparatus, synthesis, NMR spectra, crystal structures, DFT calculations and fluorescence spectra. CCDC 1486034. For ESI and crystallographic data in CIF or other electronic format see DOI: 10.1039/c6ob01695b

and catechol (CA) quenched the fluorescence by a PET mechanism.

Experimental

Materials

3-(*N*,*N*′-Dimethylamino)phenylboronic acid, formaldehyde solution, 37 wt% ACS reagent in H_2O and 4-(2-hydroxyethyl)-1-piperazineethanesulfonic acid (HEPES) were purchased from Sigma-Aldrich Japan (Tokyo, Japan). Acetic acid, dichloromethane, methanol, sodium hydrogen carbonate, hydrochloric acid, sodium oxide, D-fructose (Fru), D-glucose (Glc) and CA were purchased from Wako Pure Chemical Industries (Osaka, Japan). Cresyl violet (fluorescence reference standard) was purchased from Cosmo Bio Co., Ltd (Tokyo, Japan). All chemicals were used without further purification.

Apparatus

A reaction was monitored by thin-layer chromatography (TLC) on silica gel GF254 plates. Flash chromatography was performed with silica gel by using a YAMAZEN smart flash AI-580S. NMR spectra were recorded on a Varian 400MR. Tetramethylsilane was used as an internal standard for the ^1H and ^{13}C NMR spectra. $BF_3{\cdot}OEt_2$ was used as an external standard for ^{11}B NMR. The mass spectrum was recorded with a JEOL JMS-MStation. Elemental analysis was performed on a Yanaco MT-6 CHN analyzer. Single-crystal X-ray diffraction was measured with a Bruker APEXII CCD area-detector diffractometer. UV-Vis absorption spectra were recorded on a JASCO V-560, ETC-505T. Fluorescence spectra were recorded on a Shimadzu RF-5300PC. All calculations were carried out by using the Gaussian 09 suite of programs (Tables S2–S5 in the ESI†). All structures were optimized by using the B3LYP functional and 6-311+G(d) basis set. The solvent effect (water) was considered and simulated using the polarizable continuum model (PCM).

Synthesis of JS-R

3-(*N*,*N*′-Dimethylamino)phenylboronic acid (3.00 g, 18.2 mmol) was dissolved in AcOH (15 mL). 37% formaldehyde solution (6.8 mL, 91 mmol) was added to the above solution. The mixture was stirred for 2 hour at 85 °C. After the reaction, the mixture was cooled to room temperature and neutralized with saturated $NaHCO_3$. The reactant was extracted with CH_2Cl_2 (100 mL × 3). The organic layer was washed with brine and dried over Na_2SO_4. The solvent was removed under reduced pressure. The residue was partially purified through a silica gel column (100/0 → 0/100 CH_2Cl_2/MeOH) to provide a dark blue powder of crude JS-R. The crude was dissolved in HCl solution of pH 2 and adjusted to pH 3 with 1 M NaOH solution. After filtration, the filtrate was further adjusted to pH 2 with 1 M HCl solution and more NaCl (nearly saturated concentration) was added to the solution. The mixture was stirred for 5 hour at room temperature. 39.0 mg of the precipitate was collected as a dark blue powder of JS-R (borinic acid form) on the filter (Fig. 2a). Based on the result of elemental analysis, the purity was calculated to be 63%, and the reaction yield was 0.86%. Characterization of JS-R (borinic acid form), EI-MS: 279 (M^+ without Cl^-), ^1H NMR (400 MHz, CD_3OD): δ 7.76 (s, 1H), 7.58 (d, 2H), 7.24 (s, 2H), 6.83 (d, 2H), 3.34 (s, 12H) (Fig. S1 in the ESI†). ^{13}C NMR (100 MHz, CD_3OD): δ 161.06, 157.53, 142.73, 130.22, 119.12, 113.74, 40.87 (Fig. S2 in the ESI†), ^{11}B NMR (128 MHz, CD_3OD): 5.14 ppm (Fig. S3 in the ESI†). Elemental analysis, calculated for $C_{17}H_{24}N_2BO_3Na_{2.5}Cl_{3.5}$ [JS-R (borinic acid form)·5/2NaCl·2H_2O]: C 41.09, H 4.87, N 5.64%, found: C 41.26, H 5.00, N 5.44%.

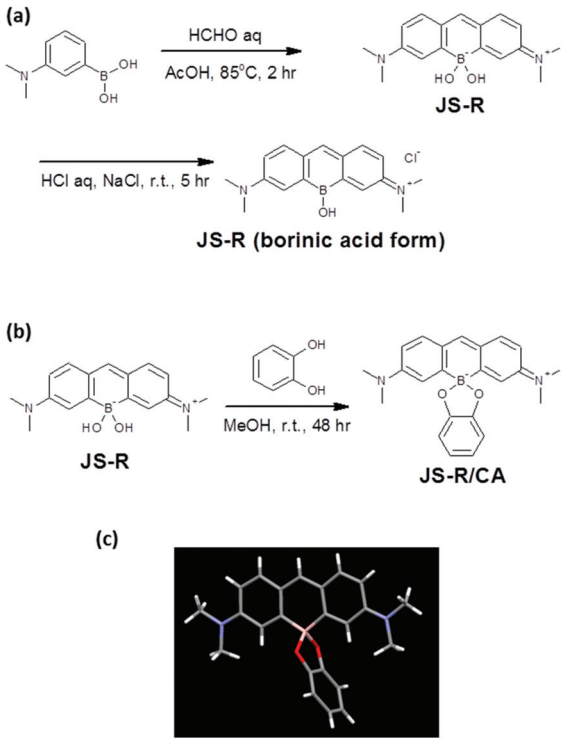

Fig. 2 (a) Synthesis of JS-R and borinic acid form of JS-R, (b) preparation of complex of JS-R and CA, (c) a single crystallography of the complex of JS-R and CA.

Crystallization of complex of JS-R and CA

The partially purified crude JS-R (48.9 mg) through a silica gel column was dissolved in methanol (5 mL). Catechol (92.9 mg) was added to the JS-R solution and left to stand for 48 hour at room temperature (Fig. 2b). Then the precipitate was collected as crystals of the JS-R/CA complex (11.4 mg) which was analysed by single X-ray crystallography (Fig. 2c).

Results and discussion

Synthesis and structural analysis of JS-R

For the synthesis of JS-R, 3-(*N*,*N*′-dimethylamino)phenylboronic acid was reacted with formaldehyde in acetic acid. After the nucleophilic addition of two aromatic rings to formalde-

hyde, a xanthene derivative was automatically formed through an elimination of one boronic acid to form the borinate centre at the 10th position and oxidation at the 9th position of the xanthene. This new reaction, forming borinate by condensing two boronic acids, is an interesting finding for C–B bond-forming chemistry.[16] The low reaction yield was due to the difficulty in the purification of the ionic product of JS-R, and it would be improved by further considering the purification conditions.

The borinic acid form of JS-R was precipitated with sodium chloride from acidic brine solution. NMR analysis of the ^{1}H, ^{13}C and ^{11}B nuclei confirmed that the precipitate (borinic acid form of JS-R) did not contain any other organic compounds (Fig. S1–3 in the ESI†). A crystal of a complex of JS-R and CA was obtained from a methanol solution, and a single-crystal structure analysis confirmed its structure (Fig. (2c), Fig. S4–7, Table S1 in the ESI†). The lengths of the B–C bonds were 1.620(4) and 1.624(4) Å, respectively. The other C–C bonds of JS-R were approximately 1.4 Å (Fig. S4 in the ESI†), which implies that there was little bond alternation in the borinic cycle moiety. Conversely, the JS-R moiety has a coplanar π-conjugated framework, in which the C–B–C angle was 112° (Fig. S5 in the ESI†). The dihedral angle between the JS-R moiety and a plane defined by the O–B–O atoms was 90° (Fig. S6 in the ESI†), and the dihedral angle between the O–B–O plane and O–C–C–O was 21° (Fig. S7 in the ESI†).

Absorption and fluorescence spectra of JS-R

JS-R shows an Abs_{max} at 611 nm and emission maxima (Em_{max}) at 631 nm when excited with 611 nm light (Fig. 3). The Abs_{max} and Em_{max} of JS-R are longer than those of PY (Abs_{max} = 552 nm, Em_{max} = 569 nm in CH_2Cl_2), which is a corresponding xanthene dye.[15] In order to reveal the reason for its optical characteristics, the Gaussian suite of programs was employed at the B3LYP/6-311+G(d) level of theory for density functional theory (DFT) calculations.[17] Although JS-R and PY have almost the same shape in the HOMO, there is a crucial difference in the LUMO on the heteroatom at the 10th position (Fig. 1a). In the LUMO of PY, the oxygen atom has a lobe whose phase is opposite to the lobes of the adjacent carbons, and thereby the aromatic π-conjugated system is completely divided by the existence of the oxygen atom, which results in the relatively high level of the LUMO. In contrast, in the LUMO of JS-R, there is no lobe on the boron atom; therefore, the existence of the sp^3 boron atom does not increase the LUMO level.

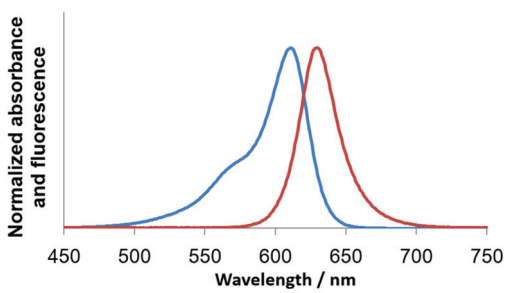

Fig. 3 Absorption and fluorescence spectra (λ_{ex} = 611 nm) of JS-R (6.3 μM) in 10 mM HEPES buffer at pH 7.4.

Response of JS-R for polyol

Note that replacing the oxygen atom with a borinate enables JS-R to act as a sugar sensor. Fig. 4(a) shows the effects of Fru on the absorption spectrum of JS-R in an aqueous buffered solution at pH 7.4. The Abs_{max} value was further shifted to a longer wavelength in the presence of Fru. CA also induced a red-shift of Abs_{max} (Fig. 4b). We conducted DFT calculations to estimate the energy gaps of the transitions of PY, JS-R and JS-R esters. Fig. 4(c) shows the HOMO–LUMO gaps of PY, JS-R and JS-R/Fru complexes. The geometries from the X-ray crystallographic structure were used initially for geometry optimisation. Some calculations were performed using the optimised structures. Hence, the optimised molecular structures of PY, JS-R and JS-R/Fru were calculated. In the optimised structure, the HOMO was on the CA moiety (Fig. 5). In the case of JS-R/CA, the (HOMO−1)–LUMO gap relating to Abs_{max} is shown in Fig. 4(c).

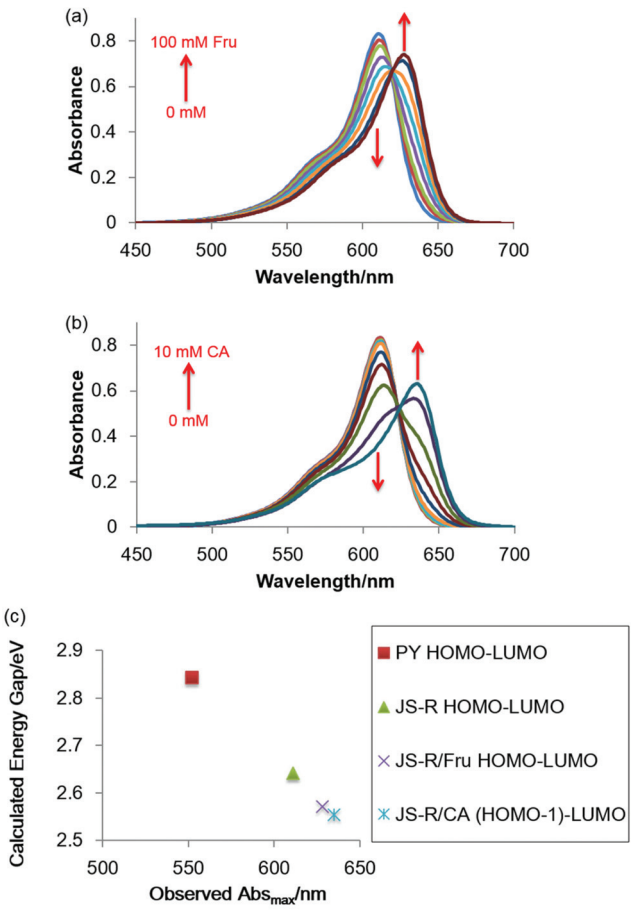

Fig. 4 Absorption spectra of JS-R (6.3 μM) in 10 mM HEPES buffer at pH 7.4; (a) the effect of Fru (0, 1, 2, 5, 10, 20, 50, 100 mM); (b) the effect of CA (0, 0.1, 0.2, 0.5, 1, 2, 5, 10 mM); (c) the relationship between observed Abs_{max} and their energy gaps.

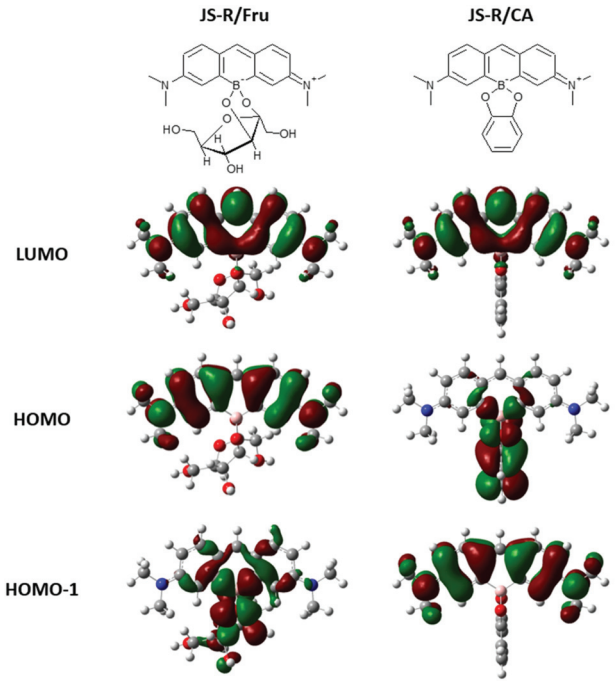

Fig. 5 Chemical structures of complexes of JS-R/Fru and JS-R/CA, and their DFT calculation results of LUMO, HOMO, and HOMO–1.

The calculated energy gaps have a good linear relationship with the measured values of Abs_{max} (Fig. 4c). In the LUMOs of JS-R/Fru and JS-R/CA, the two lobes on the carbon atoms were connected by skipping the boron atom (Fig. 5), although the two lobes of the carbon atoms in the LUMO of JS-R were not connected (Fig. 1a). The connection of the two lobes probably contributes to extend the π-conjugated system and to decrease the energy gap. Here we have proposed a novel strategy to create a sugar sensor based on borinic acid by incorporating borinate into the π-conjugated system.

The molar absorption coefficient of JS-R was measured to be 1.3×10^5 M^{-1} cm^{-1}, and its quantum yield was calculated to be 0.59 by using cresyl violet as a reference compound.[18–20] These values were comparable to PY and rhodamine derivatives,[19–21] and thus JS-R can be a good basic skeleton for fluorescent dyes. In the fluorescence spectra of JS-R, Fru addition induced a redshift of the Em_{max} and a decrease in the fluorescence intensity (Fig. 6a). Glc also showed a similar effect in the fluorescence spectra (Fig. S8 in the ESI†). By using curve-fitting analysis,[22] the binding constants are calculated to be 1.23×10^2 and 3.30 M^{-1} for Fru and Glc, respectively (Fig. S9 in the ESI†). The binding selectivity was similar to that of diphenylborinic acid.[1]

The sugar-induced decrease in the fluorescence intensity of JS-R shown in Fig. 6(a) can be explained by its decrease in absorption at 611 nm (Fig. 4a). In contrast, when JS-R was excited at 632 nm, which is the Abs_{max} in the presence of Fru and Glc, the fluorescence intensity increased (Fig. S10 in the ESI†). These results propose a wide variety of applications of JS-R with a ratiometric sensing approach. The fluorophore of

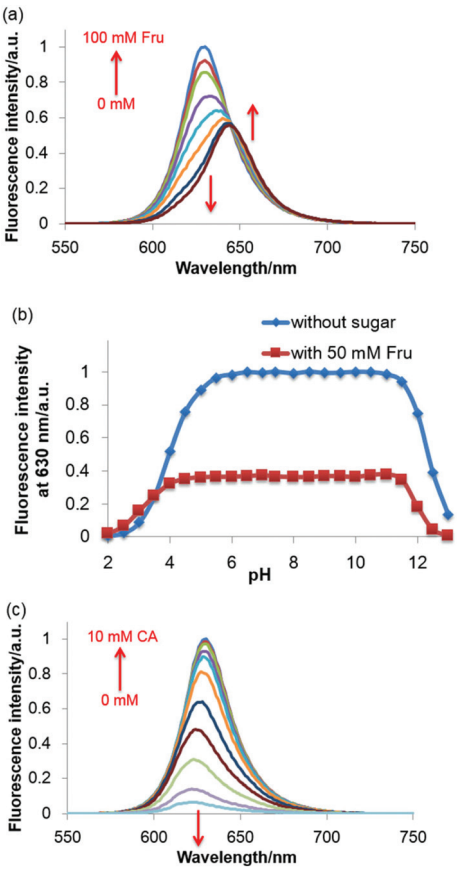

Fig. 6 Fluorescence spectra of JS-R (6.3 μM) in 10 mM HEPES buffer at pH 7.4; (a) the effect of Fru (0, 1, 2, 5, 10, 20, 50, 100 mM); (b) the effect of pH on the response; (c) the effect of CA (0, 0.1, 0.2, 0.5, 1, 2, 5, 10 mM).

JS-R itself can directly capture a diol moiety, resulting in a change in the orbital shape and spectra of absorption and fluorescence.

Previously, it has been widely discussed that the spatial arrangement of the boronic acid moiety, spacer and chromophore is important to gain a signal from a fluorophore for the ICT and PET systems. However, no one has proposed the direct incorporation of a borinic centre into a fluorophore. Borinate has two B–C bonds; therefore, incorporated borinate can form a part of the ring of the fluorophore. In contrast, boronic acid cannot bridge between two carbon atoms because boronic acid has only one B–C bond, thus boronic acid groups cannot be incorporated into but only appended to a fluorophore. We think that the C–B–C bridging by the borinate centre of JS-R is the key for the fluorescence response. Recently, Liu *et al.* have reported that *O*-BODIPY containing N–B–N bridging by sp^3 boron can directly bind sugar; however, *O*-BODIPY did not show any fluorescence change upon sugar binding.[23]

pH resistance properties of JS-R for polyol sensing ability

An additional remark which should be made here is that the sugar response of JS-R is resistant to the effect of pH

variations. Fig. 6(b) shows the pH response of fluorescence intensity in the presence and absence of 50 mM Fru. The pK_{a1} and pK_{a2} values of JS-R in the absence of sugar were calculated to be 3.99 and 12.54, respectively, with curve-fitting analysis.[22] The pK_{a1} corresponds to the equilibrium between borinic acid and borinate. The pK_{a2} is probably due to the addition of OH^- at the 9th position. We confirmed that the pH-induced changes were reversible with absorbance spectral measurements (Fig. S11 in the ESI†). Above pH 4, the major species of JS-R is the borinate form, which can interact with sugars and change the fluorescence intensity. JS-R shows substantially the same response in a wide range, from pH 5.5 to 11 (Fig. (6b), Fig. S12 in the ESI†). In this range, the fluorescence intensity was not affected by pH variation. This pH resistance of JS-R is quite unique and is usually impossible for sugar sensors based on boronic acids. Usually, pH must be adjusted when using sugar sensors based on boronic acids. One of the major signalling systems for sensors based on boronic acids is ICT.[7–9] In this type of a sensor, an sp^2 hybridised boronic acid turns into an sp^3 boronate through cyclic ester formation between the sugar and boronic acid moiety, in which there is coordination of OH^- to the boron centre simultaneously. This OH^- coordination plays a crucial role in the fluorescence change. Therefore, OH^- concentration, *i.e.* pH, should be strictly controlled for sugar sensing because a small fluctuation in pH affects the fluorescence intensity. In addition, these sensors only work in a very narrow pH range that is close to the pK_a of the boronic acid moiety. In contrast, JS-R responds to sugar without any change in the hybridisation state.

Catechol induced quenching of JS-R by the PET mechanism

In addition, JS-R shows another type of response for CA through PET. CA shows a relatively high affinity for JS-R, and the binding constant was calculated to be 1.22×10^3 M^{-1}, which is similar to that of diphenylborinic acid.[1] The fluorescence intensity decreased without a shift in the wavelength of Em_{max} as the catechol concentration increased (Fig. 6c). DFT calculations well-explained the quenching mechanism by PET. In the complex of JS-R and catechol, the HOMO exists on the catechol moiety (Fig. 5). On the other hand, the HOMO−1 and LUMO are on the JS-R moiety. When an electron of the fluorophore is excited from the HOMO−1 to the LUMO, another electron from catechol (HOMO) occupies the half-vacant HOMO−1, and the electron of the LUMO cannot return to the occupied HOMO−1, resulting in quenching of fluorescence. The quenching phenomenon by catechol promises further development of JS-R derivatives for chemical sensors based on a PET fluorescence regulation system.

Conclusion

As aforementioned, JS-R showed fluorescent changes through two different mechanisms. One of them is based on the LUMO change through the esterification reaction between JS-R and a polyol, which is quite unique to JS-R. The incorporated borinate centre provides a redshift of the fluorophore, polyol binding ability and a place for LUMO change through esterification. Another mechanism for fluorescence change is the PET, which has been widely studied with fluorescein derivatives.[24,25] Recently, Si-xanthene derivatives have attracted much attention due to their red and near-infrared fluorescence for biological applications.[19,26] It may not be difficult to apply the previous strategy utilised for xanthene derivatives to JS-R. The red fluorescence and polyol binding ability of JS-R will pave the way for new biological applications of chemical sensors. We have provided two important findings through the investigation of JS-R. One is that an internalised borinate centre is effective to extend the π-conjugation of a xanthene skeleton and to emit a red light. The other is that a borinate centre can be a novel signalling mechanism for chemical sugar sensors. The interaction between a borinate and sugar directly influences the optical properties of JS-R. We will provide many derivatives based on JS-R by replacing the group at the 9th position or substituents on the N atoms to meet a range of demands.

Notes and references

1 M. G. Chudzinski, Y. Chi and M. S. Taylor, *Aust. J. Chem.*, 2011, **64**, 1466–1469.
2 E. Dimitrijevic and M. S. Taylor, *Chem. Sci.*, 2013, **4**, 3298–3303.
3 F. Cheng, W.-M. Wan, Y. Zhou, X.-L. Sun, E. M. Bonder and F. Jäkle, *Polym. Chem.*, 2015, **6**, 4650–4656.
4 B. Wang, S. Takahashi, X. Du and J. Anzai, *Biosensors*, 2014, **4**, 243–256.
5 X. Wu, Z. Li, X.-X. Chen, J. S. Fossey, T. D. James and Y.-B. Jiang, *Chem. Soc. Rev.*, 2013, **42**, 8032–8048.
6 Y. Egawa, R. Miki and T. Seki, *Materials*, 2014, **7**, 1201–1220.
7 J. S. Hansen, J. B. Christensen, J. F. Petersen, T. Hoeg-Jensen and J. C. Norrild, *Sens. Actuators, B*, 2012, **161**, 45–79.
8 S. Arimori, L. Bosch, C. Ward and T. D. James, *Tetrahedron Lett.*, 2001, **42**, 4553–4555.
9 R. Ozawa, T. Hayashita, T. Matsui, C. Nakayama, A. Yamauchi and I. Suzuki, *J. Inclusion Phenom. Macrocyclic Chem.*, 2007, **60**, 253–261.
10 J. D. Larkin, K. A. Frimat, T. M. Fyles, S. E. Flower and T. D. James, *New J. Chem.*, 2010, **34**, 2922–2931.
11 H. Kano, D. Tanoue, H. Shimaoka, K. Katano, T. Hashimoto, H. Kunugita, S. Nanbu, T. Hayashita and K. Ema, *Anal. Sci.*, 2014, **30**, 643–648.
12 S. Arimori, M. L. Bell, C. S. Oh and T. D. James, *Org. Lett.*, 2002, **4**, 4249–4251.
13 Y. J. Huang, W. J. Ouyang, X. Wu, Z. Li, J. S. Fossey, T. D. James and Y. B. Jiang, *J. Am. Chem. Soc.*, 2013, **135**, 1700–1703.

14 Y.-J. Huang, Y.-B. Jiang, S. D. Bull, J. S. Fossey and T. D. James, *Chem. Commun.*, 2010, **46**, 8180–8182.
15 M. Fu, Y. Xiao, X. Qian, D. Zhao and Y. Xu, *Chem. Commun.*, 2008, 1780–1782.
16 M. Ingleson, *Synlett*, 2012, 1411–1415.
17 M. J. Frisch, *et al.*, *Gaussian 09, Revision A.02*, Gaussian, Inc., Wallingford CT, 2009. See the ESI.†
18 S. J. Isak and E. M. Eyring, *J. Phys. Chem.*, 1992, **96**, 1738–1742.
19 Y. Koide, Y. Urano, K. Hanaoka, T. Terai and T. Nagano, *ACS Chem. Biol.*, 2011, **6**, 600–608.
20 Q. A. Best, A. E. Johnson, B. Prasai, A. Rouillere and R. L. McCarley, *ACS Chem. Biol.*, 2015, **11**, 231–240.
21 M. Beija, C. A. M. Afonso and J. M. G. Martinho, *Chem. Soc. Rev.*, 2009, **38**, 2410–2433.
22 C. J. Ward, P. Patel and T. D. James, *J. Chem. Soc., Perkin Trans. 1*, 2002, 462–470.
23 B. Liu, N. Novikova, M. C. Simpson, M. S. M. Timmer, B. L. Stocker, T. Söhnel, D. C. Ware and P. J. Brothers, *Org. Biomol. Chem.*, 2016, **14**, 5205–5209.
24 K. Tanaka, T. Miura, N. Umezawa, Y. Urano, K. Kikuchi, T. Higuchi and T. Nagano, *J. Am. Chem. Soc.*, 2001, **123**, 2530–2536.
25 Y. Urano, M. Kamiya, K. Kanda, T. Ueno, K. Hirose and T. Nagano, *J. Am. Chem. Soc.*, 2005, **127**, 4888–4894.
26 K. Hirabayashi, K. Hanaoka, T. Takayanagi, Y. Toki, T. Egawa, M. Kamiya, T. Komatsu, T. Ueno, T. Terai, K. Yoshida, M. Uchiyama, T. Nagano and Y. Urano, *Anal. Chem.*, 2015, **87**, 9061–9069.